RSC Advances

PAPER

View Article Online
View Journal | View Issue

Cite this: *RSC Adv.*, 2014, **4**, 6685

Evaluation of decomposition products of EMImCl·1.5AlCl$_3$ during aluminium electrodeposition with different analytical methods

Sandra Poetz,* Patricia Handel, Gisela Fauler, Bernd Fuchsbichler, Martin Schmuck and Stefan Koller

Received 30th October 2013
Accepted 3rd January 2014

DOI: 10.1039/c3ra46249h

www.rsc.org/advances

Ionic liquids are of great importance for electrodeposition of metals, which can't be deposited from aqueous electrolytes due to their negative standard potentials. In this paper non-woven polymers were coated with aluminium by electrodeposition from 1-ethyl-3-methyl-imidazolium chloride and subsequently established as 3D current collectors for lithium-ion batteries. We investigated the long-term stability of the ionic liquid (IL) for electrodeposition of aluminium under process-oriented conditions. The degradation products were analysed by headspace gas chromatography-mass spectrometry, pyrolysis-gas chromatography-mass spectrometry (Py-GC/MS) and ^{1}H/^{13}C nuclear magnetic resonance spectroscopy (NMR). The main decomposition products derived from thermal degradation, especially from cleavage of an alkyl chain and were identified as chloromethane, dichloromethane, methylimidazole, ethylimidazole and deprotonated 1-ethyl-3-methylimidazole.

Introduction

The application of room temperature ionic liquids (RTIL) as electrolyte systems for electrochemical reactions has received a lot of attention during the last few decades. Due to their attractive properties such as a high thermal stability, high ionic conductivity, wide electrochemical window, negligible vapour pressure, low melting point and their adjustability for tailored applications[1,2] ionic liquids are being studied for use in batteries,[3] electroplating[4] and many other fields.

Because of its low price, good electric conductivity and the ability to form a protective passive surface layer, aluminium is considered to be the metal of choice as current collector for high voltage applications (>3.5 V *vs.* Li/Li$^+$) in lithium-ion batteries (LIBs).[5] Conventional current collectors for LIBs are composed of two-dimensional, flat metal foils. However, three-dimensional current collectors could provide several advantages like the possibility of higher mass loadings without delamination of electrode material or enhanced electrolyte penetration due to a higher surface area.[6]

In this work, we developed a 3D current collector for the positive electrode of lithium-ion batteries, based on a non-woven polymer, which was plated with a thin Ni-layer by chemical reduction and subsequently electrodeposition of an aluminium layer from ionic liquid.

There are several methods recorded for coating workpieces with aluminium, like thermal spray coating, hot dipping, physical and chemical vapour deposition (PVD, CVD) or electroplating.[4,7] Due to the negative standard potential of aluminium, the electrodeposition is not feasible from aqueous media owing to cathodic hydrogen evolution. On this account electrolytes have to be aprotic and only molten salts and organic electrolytes are suitable for aluminium electrodeposition.[8]

As a matter of fact, ionic liquids offer several beneficial properties compared to organic electrolytes, like negligible vapour pressure at elevated temperatures and higher intrinsic electrical conductivity.[1,9] Based on this considerations, we decided to use the ionic liquid 1-ethyl-3-methyl-imidazolium chloride (EMImCl) mixed with $AlCl_3$ in the ratio 1 : 1.5 for our studies.

However, ionic liquids tend to decompose after being exposed to elevated temperatures, catalytically active molecules or the influence of an electric field.[10,11] Beside the continuous loss of ionic liquid the resulting decomposition products can change the desired physico-chemical properties and may impact plating process as well. The deterioration of the plating bath is an irreversible process involving several factors beside decomposition of the organic molecules of the IL. In the special case of EMImCl·1.5AlCl$_3$, $AlCl_3$ is consumed during electroplating. Since Al can only be deposited from so called "acidic" solutions which contain an excess of $[Al_2Cl_7^-]$ ions over Cl^-, the plating bath will shift to "neutral" or "basic" composition through consumption of $AlCl_3$.[1,12]

The thermal and electrochemical stability of imidazolium-based ionic liquids and their decomposition products have been studied in a number of papers using different analytical methods like thermogravimetry (TG),[13] pyrolysis-gas chromatography,[14] liquid chromatography-mass spectrometry (LC-MS)[10]

VARTA Micro Innovation GmbH, Stremayrgasse 9, A-8010 Graz, Austria. E-mail: s.poetz@vartamicroinnovation.at; Fax: +43 (316) 873 32387; Tel: +43 (316) 873 32353

and nuclear magnetic resonance spectroscopy (NMR).[15,16] In our present work we focus on the determination of thermal and electrochemical degradation products of EMImCl·1.5$AlCl_3$ during electroplating by headspace GC/MS, Py-GC/MS and NMR studies.

Experimental

Preparation of the 3-dimensional current collector for LIBs

The Ni–P films were deposited on non-woven PE, with dimensions of 20 mm × 20 mm × 0.15 mm, pretreated in a basic cleaning solution at 338 K for 5 min, 30% HCl etching for 60 s at room temperature and $PdCl_2$ activation for 60 s at 313 K. In between all steps, the substrates were rinsed with deionised water. Subsequently, Ni–P films were electrolessly deposited on pretreated substrates. Nickel films were deposited from baths containing 3.5 g L^{-1} Ni^{2+} ions and sodium hypophosphite as reducing agent. The electrolyte for Ni–P deposition was composed of $NiSO_4 \cdot 6H_2O$, $NaH_2PO_4 \cdot H_2O$ and NH_3. Operating temperature and pH of the baths was set to 338 K and 9, respectively. All baths were supplied by Enthone, Cookson Electronics and were used as received without further purification.

For electrodeposition of aluminium, the bath was composed of 1-ethyl-3-methylimidazolium chloride (EMImCl–$AlCl_3$ molar ratio 1 : 1.5), supplied by BASF (Basionics™ Al01), and used as received without further purification. All chemicals were handled under argon atmosphere in a glove box, in which the moisture and oxygen content was maintained below 0.1 ppm. The electrodeposition was performed in an electrochemical cell (100 mL) with a three-electrode arrangement using an Autolab PGSTAT 100 & 10 A Booster under inert gas conditions. The deposits were obtained by operating in current controlled (galvanostatic) conditions at 368 K, using pure aluminium rods (Goodfellow 99 999%) as counter and reference electrodes. As substrates for electrodeposition, nickel plated polymer non-wovens with dimensions of 20 mm × 20 mm × 0.15 mm were used.

Headspace GC/MS and Py-GC/MS measuring conditions

A Frontier Laboratory PY2020iD pyrolyser was directly attached to the injection port of a gas chromatograph (GC, Agilent 7890 A) equipped with a metal capillary column and an Agilent 5975 C VLMSD mass spectrometer as detector. Helium was used as carrier gas. For identification of the decomposition products, the MS system was utilised in electron ionisation mode at 70 eV. The mass scan range was set between m/z 15 and 300. About 10 μL of the electrolyte for aluminium deposition was placed in a small sample cup and then inserted into the heated centre of the pyrolyser furnace at 368 K, and this temperature held for 1 h. Afterwards, the pyrolysis technique was switched into the evolved gas analysis (EGA) mode, heating the pyrolyser furnace to 853 K, the decomposition products were transferred into the mass spectrometer continuously. The flow rate was set to 1 mL min^{-1}, the heat rate was 20 K min^{-1} and the split ratio was 1 : 100. Headspace GC/MS analysis of the sample headspace was carried out using a HP5-MS column (5% phenyl methyl silox Agilent) as stationary phase for separation.

The inlet temperature was set to 523 K and the injection was performed manually (split ratio of 1 : 500). The temperature program started at 313 K, increased to 453 K with 10 K min^{-1} held for 1 min. The mass scan range was set between m/z 20 and 100.

NMR studies

The chloroaluminate molten salts were measured with a D_2O capillary without any solvent and pure EMImCl was dissolved in $CDCl_3$. The samples for NMR measurement were prepared in an argon filled glove box. The ^1H and ^{13}C NMR spectra were recorded with a Varian Mercury 300 MHz spectrometer using tetramethylsilane as reference, at 300.224 MHz and 75.499 MHz respectively. All NMR spectra were recorded at 298 K.

Conductance measurement

A Knick 703 conductivity meter was used for the determination. The conductivity of the samples was determined within a temperature range of 293 K to 368 K divided into 10 K steps. The cell constant was determined using aqueous 0.1 mol L^{-1} NaCl solution. The temperature of the samples was controlled by a Julabo F32 thermostat. The cell for conductivity measurement was assembled in an argon filled glove box and then carefully sealed.

Morphology analysis

Morphology analysis was performed using a Tescan Vega3 scanning electron microscope (SEM) equipped with an energy dispersive X-ray detector (Oxford Instruments INCAx-act) for determination of elemental composition of the coating.

Results and discussion

Electrochemical deposition and measurement

A typical voltammogram for deposition and stripping of aluminium on nickel plated non-woven polymer from EMImCl·1.5$AlCl_3$ ionic liquid at 368 K is shown in Fig. 1. The

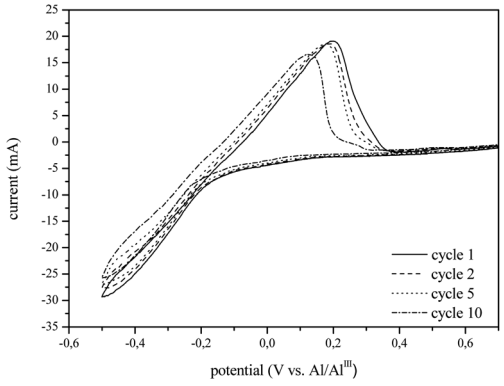

Fig. 1 Cyclic voltammogram of aluminium deposition and dissolution on nickel plated polymer fibres in EMImCl·1.5$AlCl_3$; scan rate: 10 mV s^{-1}.

cathodic and anodic peaks, beginning at −0.2 V and 0.1 V (*vs.* Al/Al^{3+}) respectively, can be attributed to the reversible deposition and dissolution of aluminium and correlates with already published data in literature.[17,18] Interestingly, the reduction and oxidation potentials of $Al_2Cl_7^-$ slightly shift to more negative potentials with ongoing cycling (Fig. 1).

The morphology of the electroplated aluminium layer depends on the applied current density and the temperature.[19–22] As revealed in our experimental work, a current yield above 90% could be achieved at 368 K, indicating, that side reactions could be kept to a minimum. Therefore, the mass of the deposited aluminium layer could be calculated according to Faraday's law.

Fig. 2 illustrates the conductivities of untreated 1-ethyl-3-methyl-imidazolium chloride compared to thermally stressed and electrochemically aged ionic liquid. As shown in Fig. 2, thermal and electrochemical treatment seems to have no significant effect on the conductivity of the electrolyte. Aluminium deposition from $EMImCl \cdot 1.5AlCl_3$ at room temperature occurs only slowly and could be explained by the reduced conductivity of the electrolyte at room temperature compared to higher temperatures (Fig. 2). It should be noted that this behaviour could originate from slow kinetics of the electrode reaction itself as well. The resulting aluminium layer and the current yield from electrodeposition at room temperature are very bad.

By using a current density of 10 mA cm^{-2} at 368 K, a rough aluminium layer with a high surface area is obtained (Fig. 3a). The surface of the deposited aluminium layer becomes smoother, when the applied current density has been increased during deposition, as can be seen in Fig. 3b. For application as current collector in lithium-ion batteries, a high surface area is desirable, because increasing the contact area between the active material and the current collector would decrease the inner cell resistance significantly and improves the adhesion of the active material additionally.

The EDX spectrum after aluminium electrodeposition (Fig. 4) shows a pure aluminium layer. The detected oxygen could be attributed to passivation of aluminium on air during the transfer of the sample to the vacuum chamber of the SEM.

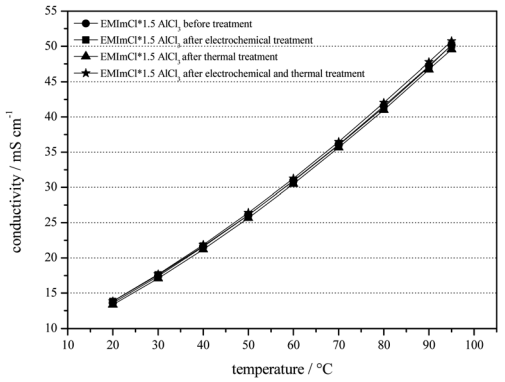

Fig. 2 Conductivities of $EMImCl \cdot 1.5AlCl_3$ before and after treatment.

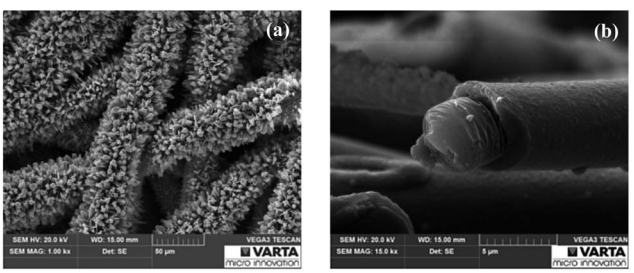

Fig. 3 SEM images of with aluminium plated polymer fibres; current density: 10 mA cm^{-2} (a) and 20 mA cm^{-2} (b).

Determination of the electrochemical and thermal decomposition products of $EMImCl \cdot 1.5AlCl_3$

Fig. 5 illustrates the thermal degradation pathways of EMImCl based on literature.[10] The most abundant decomposition products during thermal treatment of the ionic liquids are imidazole derivates and alkylated anions as can be seen in reaction (1). Either one alkyl chain can be abstracted or even both.[11] Other considerable decomposition products are diethyl- or dimethyl imidazole, which will be formed during re-alkylation of a dealkylated cation, or by direct exchange of the alkyl chains of two cations (Fig. 5(2)).[10,23] A further possibility for decomposition reaction is the deprotonation of the C2-atom by strong nucleophiles, which results in the formation of carbenes (3). Carbenes are reactive components and can react with other molecules of the ionic liquid or any present dissolved decomposition products.[24,25]

Possible electrochemical decomposition products of 1-ethyl-3-methylimidazolium chloride are shown in Fig. 6. In electrochemical processes, 1,3-dialkylimidazolium radicals are formed in analogy to carbenes. These radicals can react with each other to form neutral molecules (radical–radical coupling).[26]

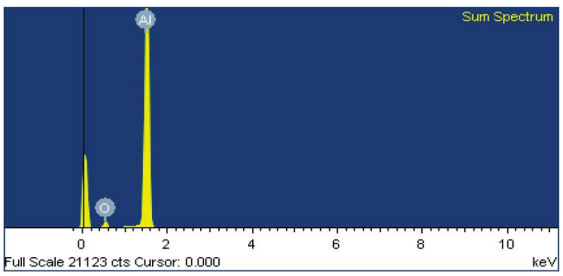

Fig. 4 EDX spectrum of aluminium plated polymer fibres.

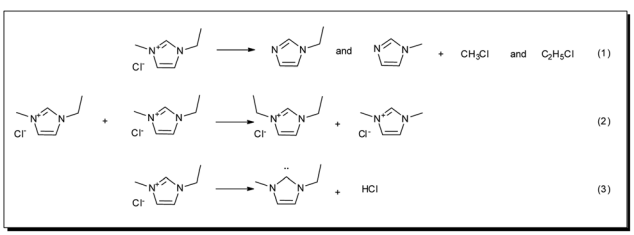

Fig. 5 Thermal decomposition mechanism of 1-ethyl-3-methyl-imidazolium chloride.[10]

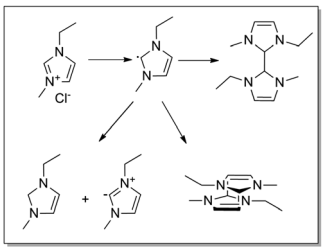

Fig. 6 Electrochemical decomposition mechanism of 1-ethyl-3-methylimidazolium chloride.[26]

It is very important to mention that humidity-sensitive species, like $AlCl_3$, will undergo hydrolysis even with traces of water. Halogenaluminates show strong exothermic reactions with water and decompose to aluminium oxides and aluminium hydroxides, while releasing HX.[12]

In this work, a methodic approach was developed to identify decomposition products of 1-ethyl-3-methylimidazolium chloride in combination with $AlCl_3$, using head-space gas chromatography-mass spectrometry, pyrolysis gas chromatography-mass spectrometry analysis and NMR studies. Samples of the complexed ionic liquid were treated thermally and electrochemically, respectively.

An electrochemical cell was filled with a certain amount of electrolyte, fitted with a nickel-plated polymer as working electrode and aluminium wires as counter- and reference electrode. The cell was assembled and sealed under argon atmosphere. For thermal stress only, EMImCl·1.5$AlCl_3$ was heated to 368 K and the temperature was held for 100 hours. For electrochemical treatment, the aluminium deposition was carried out at constant voltage mode with −0.1 V *vs.* Al/Al^{3+} at ambient temperature and at 368 K for 100 hours. These samples were prepared for NMR analysis in an argon-filled glove box afterwards.

For determination of volatile decomposition products of the electrolyte static head-space GC/MS analysis was carried out. Therefore, the EMImCl·1.5$AlCl_3$ sample was thermally aged at 368 K for 100 h in a glass vial fitted with a septum. Samples (4.0 mL) of the gaseous phase were taken, using a 10 mL gas-tight syringe (Hamilton) and subsequently injected into the gas chromatograph system. Chloromethane, dichloromethane and hydrochloric acid could be identified as volatile decomposition products after thermal treatment of EMImCl·1.5$AlCl_3$ at 368 K (Fig. 7). The silicon compound with a retention time of 2.10 min. originates from the reaction of chlorine with the stationary phase of the column.

For Py-GC/MS analysis fresh EMImCl·1.5$AlCl_3$ was dropped into a small-sized vertical furnace. The temperature was set to 368 K for one hour after which time the evolved gas was analysed. The results of Py-GC/MS indicate that chloromethane, hydrochloric acid, methylimidazole, ethylimidazole and deprotonated ethyl-methylimidazole (Fig. 8a) are the main thermal decomposition products of the complexed ionic liquid. No products reflecting decomposition of the imidazole rings at this temperature could be found in the thermogram. Extracted ion pyrograms are shown in Fig. 8a. The mass spectra of the certain degradation products of the ionic liquid (Fig. 8b) show typical fragmentation patterns of imidazole[27] and could therefore be identified. The mass spectrum allocated to Fig. 8b includes peaks with high masses (*m*/*z* 193 and *m*/*z* 207) and could be assigned to injection liner bleeding due to massive HCl development during sample degradation. The origin of the peak with *m*/*z* 179 couldn't be clarified yet.

For NMR studies, the samples were prepared in an argon filled glove box without any solvent (D_2O capillaries) except for the measurement of thermally treated pure EMImCl, which was dissolved in $CDCl_3$. ^1H and ^{13}C NMR spectra of the fresh, untreated EMImCl·1.5$AlCl_3$ were also recorded (Table 1).

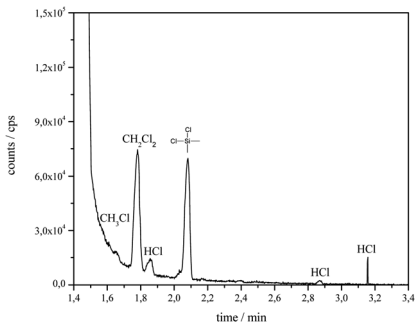

Fig. 7 Chromatogram of the decomposition products of thermally stressed EMImCl·1.5$AlCl_3$ after headspace GC/MS analysis.

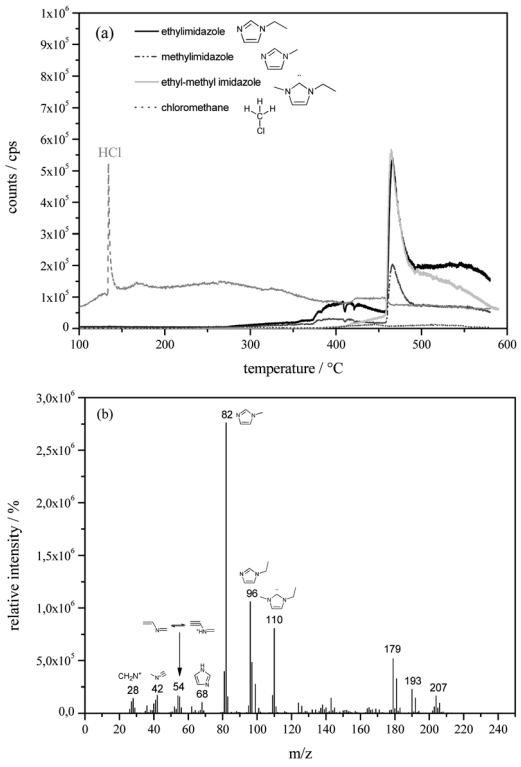

Fig. 8 Extracted ion thermograms of chloromethane, hydrochloric acid, methylimidazole, ethylimidazole and ethyl-methylimidazole (a) and the accompanied mass spectra (b).

Table 1 ^{1}H NMR data (300 MHz, D_2O) for EMImCl·1.5$AlCl_3$ and EMImCl (300 MHz, $CDCl_3$) before and after electrochemical and/or thermal treatment

Sample		t, 3H	s	s	s, 3H	q, 2H	s, 1H	s, 1H	s, 1H
1[a]	ppm	1.03	—	—	3.42	3.73	6.83	6.87	7.85
2[b]	ppm	0.91	2.12	—	3.30	3.62	6.71	6.76	7.73
3[c]	ppm	1.08	—	3.00	3.46	3.78	6.88	6.92	7.89
4[d]	ppm	1.01	2.30	2.91	3.39	3.71	6.81	6.85	7.82
5[e]	ppm	1.01	2.29	2.58	3.40	3.71	6.81	6.86	7.83
6[f]	ppm	1.30	—	—	3.82	4.13	7.44	7.44	10.16

[a] EMImCl·1.5$AlCl_3$ before treatment. [b] EMImCl·1.5$AlCl_3$ after thermal treatment at 368 K. [c] EMImCl·1.5$AlCl_3$ after electrochemical and thermal treatment at 368 K for 10 h. [d] EMImCl·1.5$AlCl_3$ after electrochemical and thermal treatment at 368 K for 50 h. [e] EMImCl·1.5$AlCl_3$ after electrochemical and thermal treatment at 368 K for 100 h. [f] EMImCl after thermal treatment at 368 K for 100 h.

EMImCl·1.5$AlCl_3$ (before treatment). ^{13}C NMR, (D_2O): δ 14.81 (s, CH_3), 36.53 (s, CH_3), 45.11 (s, CH_2), 121.84 (s, 1C), 123.53 (s, 1C), 134.11 (s, 1C) ppm.

Although EMIm halides (Cl^-, Br^- or I^-) exhibit temperatures for onset decomposition between 553 K and 583 K,[28] we have found additional peaks in the ^{1}H-spectra of the thermally treated sample at 368 K. A possible explanation could be the thermal decomposition of the complexed ionic liquid indicating the presence of alkyl chlorides and HCl in the thermal stressed sample. On the other hand the ^{13}C-NMR spectra don't show additional peaks, but this could be due to a less sensitiveness of the ^{13}C-NMR compared to ^{1}H-NMR or GC/MS analysis. According to literature, heating of EMImCl at 373 K does not increase the imidazole content in the sample, which can be an indication for decomposition of alkylated imidazoles.[23] In our observations there are no additional peaks in the ^{1}H-spectra of heat treated EMImCl without $AlCl_3$ (Table 1). It seems that $AlCl_3$ initiates the decomposition of the IL and decreases its onset temperature dramatically. On the other hand, in the electrochemically treated sample at room temperature, no additional peaks could be observed in the NMR spectra of the electrolyte. However, the electrochemically stressed samples at elevated temperatures (368 K) show these additional peaks and are in agreement with this theory. In further consequence, $AlCl_3$ can be deemed as the crucial factor for degradation of 1-ethyl-3-methyl-imidazolium chloride used for aluminium electrodeposition at elevated temperatures, which would be optimised conditions in terms of electroplating.

Conclusions

In conclusion we successfully deposited aluminium on a non-woven polymer from an ionic liquid for application as 3D current collector for the positive electrode in lithium-ion batteries. During aluminium deposition from the imidazolium based ionic liquid, thermal degradation, initiated by $AlCl_3$, could be figured out to be the main reason for electrolyte aging. No evidence for electrochemical decomposition of this electrolyte could be found. The presented analytical approach, combining pyrolysis chromatography coupled with mass spectrometry incorporated and headspace gas chromatography-mass spectrometry enables the identification of decomposition products of ionic liquids. Thermal degradation of EMImCl·1.5$AlCl_3$ produces chloromethane, dichloromethane, hydrochloric acid, imidazole, alkylimidazole and 1-ethyl-3-methylimidazole based on the formation of a reactive carbene intermediate. Cl^- ions are irreversibly consumed and the obtained data can be explained by an equilibrium, shifts from excess of reducible Al-species $[Al_2Cl_7]^-$ to excess of the not reducible Al-compound $[AlCl_4]^-$. Another consideration that has to be taken into account is the potential drift to more negative potentials during electroplating, until the limit of the electrochemical stability window of IL is exceeded. All these factors will contribute to irreversible decomposition of ionic liquid and damage of the plating bath.

Acknowledgements

The authors acknowledge the Austrian Research Promotion Agency (FFG) for the financial support under contract 821964 (Neue Energien 2020, Neuartige Lithium Ionen Batterie Elektroden).

References

1 T. Welton, *Chem. Rev.*, 1999, **99**, 2071–2083.
2 K. Haerens, E. Matthijs, K. Binnemans and B. Van der Bruggen, *Green Chem.*, 2009, **11**, 1357–1365.
3 A. Fernicola, B. Scorsati and H. Ohno, *Ionics*, 2006, **12**, 95–102.
4 Y. Zhao and T. J. VanderNoot, *Electrochim. Acta*, 1997, **42**, 3–13.
5 S.-T. Myung, Y. Sasaki, S. Sakurada, Y.-K. Sun and H. Yashiro, *Electrochim. Acta*, 2009, **55**, 288–297.
6 L. Hu, F. La Mantia, H. Wu, X. Xie, J. McDonough, M. Pasta and Y. Cui, *Adv. Energy Mater.*, 2011, **1**, 1012–1017.
7 *Corrosion*, ed. L. L. Shreir, R. A. Jarman and G. T. Burstein, Butterworth-Heinemann, UK, 3rd edn, 1994.
8 W. Simka, D. Puszczyk and G. Nawrat, *Electrochim. Acta*, 2009, **54**, 5307–5319.
9 J. G. Huddleston, A. E. Visser, W. M. Reichert, H. D. Willauer, G. A. Broker and R. D. Rogers, *Green Chem.*, 2001, **3**, 156–164.
10 P. Keil, M. Kick and A. König, *Chem. Ing. Tech.*, 2012, **84**, 859–866.
11 Y. Hao, J. Peng, S. Hu, J. Li and M. Zhai, *Thermochim. Acta*, 2010, **501**, 78–83.
12 A. à. K. Abdul Sada, A. M. Greenway, K. R. Seddon and T. Welton, *Org. Mass Spectrom.*, 1993, **28**, 759–765.
13 M. Kosmulski, J. Gustafsson and J. B. Rosenholm, *Thermochim. Acta*, 2004, **412**, 47–53.
14 H. Ohtani, S. Ishimura and M. Kumai, *Anal. Sci.*, 2008, **24**, 1335–1340.
15 A. G. Advent, P. A. Chaloner, M. P. Day, K. R. Seddon and T. Welton, *J. Chem. Soc., Dalton Trans.*, 1994, 3405–3413.
16 L. Xiao and K. E. Johnson, *J. Electrochem. Soc.*, 2003, **150**, E307–E311.

17 E. Perre, L. Nyholm, T. Gustafsson, P.-L. Taberna, P. Simon and K. Edström, *Electrochem. Commun.*, 2008, **10**, 1467–1470.
18 S. Z. El Abedin and F. Endres, *Acc. Chem. Res.*, 2007, **40**, 1106–1113.
19 D. Pradhan, D. Mantha and R. G. Reddy, *Electrochim. Acta*, 2009, **54**, 6661–6667.
20 G. Yue, X. Lu, Y. Zhu, X. Zhang and S. Zhang, *Chem. Eng. J.*, 2009, **147**, 79–86.
21 S. Z. El Abedin, E. M. Moustafa, R. Hempelmann, H. Natter and F. Endres, *ChemPhysChem*, 2006, **7**, 1535–1543.
22 J.-K. Chang, S.-Y. Chen, W.-T. Tsai, M.-J. Deng and I.-W. Sun, *Electrochem. Commun.*, 2007, **9**, 1602–1606.
23 N. Meine, F. Benedito and R. Rinaldi, *Green Chem.*, 2010, **12**, 1711–1714.
24 P. Bonhôte, A.-P. Dias, N. Papageorgiou, K. Kalyanasundaram and M. Grätzel, *Inorg. Chem.*, 1996, **35**, 1168–1178.
25 A. J. Arduengo and R. Krafzcyk, *Chem. Unserer Zeit*, 1998, **32**, 6–14.
26 M. C. Kroon, W. Buijs, C. J. Peters and G.-J. Witkamp, *Green Chem.*, 2006, **8**, 241–245.
27 A. Sala, F. Ferrario and E. Rizzi, *Rapid Commun. Mass Spectrom.*, 1992, **6**, 388–393.
28 A. Chowdhury and S. T. Thynell, *Thermochim. Acta*, 2006, **443**, 159–172.